

Turbulent magnetic Prandtl number and magnetic diffusivity quenching from simulations

T. A. Yousef¹, A. Brandenburg² and G. Rüdiger³

¹ Department of Energy and Process Engineering, Norwegian University of Science and Technology, Kolbjørn Hejes vei 2B, N-7491 Trondheim, Norway

² NORDITA, Blegdamsvej 17, DK-2100 Copenhagen Ø, Denmark

³ Astrophysical Institute Potsdam, An der Sternwarte 16, D-14482 Potsdam, Germany

Astron. Astrophys. 411, 321-327 (2003)

Received 21 February 2003 / Accepted 25 August 2003, Revision: 1.51

Abstract. Forced turbulence simulations are used to determine the turbulent kinematic viscosity, ν_t , from the decay rate of a large scale velocity field. Likewise, the turbulent magnetic diffusivity, η_t , is determined from the decay of a large scale magnetic field. In the kinematic regime, when the field is weak, the turbulent magnetic Prandtl number, ν_t/η_t , is about unity. When the field is nonhelical, η_t is quenched when magnetic and kinetic energies become comparable. For helical fields the quenching is stronger and can be described by a dynamical quenching formula.

Key words. magnetohydrodynamics (MHD) – turbulence

1. Introduction

The concept of turbulent diffusion is often invoked when modeling large scale flows and magnetic fields in a turbulent medium. Turbulent magnetic diffusion is similar to turbulent thermal diffusion which characterizes the turbulent exchange of patches of warm and cold gas. This concept is also applied to turbulent magnetic diffusion which describes the turbulent exchange of patches of magnetic field with different strengths and direction. Reconnection of magnetic field lines is not explicitly required, but in the long run unavoidable if the magnetic power spectrum is to decrease toward small scales. The idea of Prandtl is that only the energy carrying eddies contribute to the mixing of large scale distributions of velocity and magnetic field structures. This leads to a turbulent magnetic diffusion coefficient $\eta_t \approx \frac{1}{3}U\ell$, where U is the typical velocity and ℓ the scale of the energy carrying eddies. For the kinematic turbulent viscosity one expects similar values. Analytic theory based on the quasilinear approximation also produces similar (but not identical) values of η_t and ν_t (e.g. Kitchatinov et al. 1994).

It is usually assumed that the values of η_t and ν_t are independent of the molecular (microscopic) viscosity and magnetic diffusivity, ν and η . However, in the context of the geodynamo or in laboratory liquid metals the microscopic magnetic Prandtl number, $P_m = \nu/\eta$ is very small ($\approx 10^{-5}$). This has dramatic consequences for the mag-

netorotational instability (Balbus & Hawley 1991). This instability is generally accepted as the main mechanism producing turbulence in accretion discs (Balbus & Hawley 1998). For sufficiently small values of P_m , however, this instability is suppressed (Rüdiger & Shalybkov 2002). On the other hand, the Reynolds number of the flow is quite large ($10^5 \dots 10^6$) and the flow therefore most certainly turbulent. This led Noguchi et al. (2002) to invoke a turbulent kinematic viscosity, ν_t , but to retain the microscopic value of η . The resulting *effective* magnetic Prandtl number they used was 10^{-2} – big enough for the magnetorotational instability to develop. One may wonder, of course, why one should not instead use turbulent values for both coefficients, i.e. $\nu_t/\eta_t \approx 1$. This would lead to even more favorable conditions for the magnetorotational instability (Rüdiger et al. 2002).

Similar constraints have also been reported for the convection-driven geodynamo: Christensen et al. (1999) found that there is a minimum value of P_m of about 0.25 below which dynamo action does not occur at all. Similar results have also been reported by Cattaneo (2003). These results are disturbing, because both for the sun and for the earth, $P_m \ll 1$. For P_m of order unity, on the other hand, earth-like magnetic configurations can more easily be reproduced (see Kutzner & Christensen 2002).

Because of these restrictions, one wonders whether the effective magnetic Prandtl number to be used is not P_m , but rather the turbulent value, $P_{m,t} = \nu_t/\eta_t$. This raises

the important questions whether $P_{m,t}$ is actually of order unity and whether it is independent of the microscopic value, P_m . The aim of this paper is to estimate the value of $P_{m,t}$ using turbulence simulations.

The knowledge of the value of $P_{m,t}$ is also important for the solar dynamo. The qualitative properties of the dynamo depend on the relative importance of the large scale flows and hence on the magnitude of η_t . If η_t is too large, the influence of a meridional flow of say 10 m/s is small so that only little modification can be expected for the basic $\alpha\Omega$ -dynamo (Roberts & Stix 1972). In this case, however, we know that conventional dynamo models of the solar activity cycle have difficulty to explain Spörer's law of equatorward sunspot migration. The alternative that the resulting poleward migration can be overcompensated by an internal equatorward flow requires a sufficiently small value of η_t , which implies that $P_{m,t} > 1$ (Choudhuri et al. 1995; Dikpati & Charbonneau 1999; Bonanno et al. 2002).

Given the importance of the value of the turbulent magnetic Prandtl number it is useful to assess the problem using three-dimensional simulations of turbulent flows. We determine ν_t and η_t by measuring the decay rate of a large scale (mean) velocity and magnetic field, $\bar{\mathbf{u}}$ and $\bar{\mathbf{B}}$, respectively. We emphasize that we are not addressing the question whether ν_t and η_t can really be used in studies of the dynamo or the magnetorotational instability, for example.

We consider weakly compressible nonhelically forced turbulence and use a model similar to that of Brandenburg (2001), but with kinetic helicity fluctuating about zero. Dynamo action for such a model has recently been considered by Haugen et al. (2003), but it sets in only at magnetic Reynolds numbers above ~ 30 , which is not the case in the present simulations. We begin however by first reviewing the basic results for the values of ν_t and η_t within the framework of the quasilinear (Roberts & Soward 1975, Rüdiger 1989) and other approximations.

2. Results from quasilinear approximation

For steady homogeneous isotropic turbulence the correlation tensor is independent of \mathbf{x} and t , i.e.

$$\langle u'_i(\mathbf{x}, t) u'_j(\mathbf{x} + \boldsymbol{\xi}, t + \tau) \rangle = Q_{ij}(\boldsymbol{\xi}, \tau), \quad (1)$$

where angular brackets denote an ensemble average and primes fluctuations about the average. In the quasilinear approximation the transport coefficients are conveniently expressed in terms of the Fourier transformed correlation tensor, $\hat{Q}_{ij}(\mathbf{k}, \omega)$, which is normalized such that

$$Q_{ij}(\boldsymbol{\xi}, \tau) = \iint \hat{Q}_{ij}(\mathbf{k}, \omega) e^{i(\mathbf{k} \cdot \boldsymbol{\xi} - \omega \tau)} d\mathbf{k} d\omega. \quad (2)$$

For the turbulent viscosity and the turbulent magnetic diffusivity one finds respectively (Rüdiger 1989)

$$\nu_t = \frac{4}{15} \iint \frac{\nu^3 k^6 \hat{Q}_{ll}(\mathbf{k}, \omega)}{(\omega^2 + \nu^2 k^4)^2} d\mathbf{k} d\omega, \quad (3)$$

$$\eta_t = \frac{1}{3} \iint \frac{\eta k^2 \hat{Q}_{ll}(\mathbf{k}, \omega)}{\omega^2 + \eta^2 k^4} d\mathbf{k} d\omega. \quad (4)$$

Obviously, both quantities are of the same order of magnitude, but they are not identical. In the limits $\nu, \eta \rightarrow 0$ the expressions are drastically simplified, i.e.

$$\nu_t = \frac{1}{15} \int_{-\infty}^{\infty} \langle \mathbf{u}'(\mathbf{x}, t) \cdot \mathbf{u}'(\mathbf{x}, t + \tau) \rangle d\tau \quad (5)$$

and

$$\eta_t = \frac{1}{6} \int_{-\infty}^{\infty} \langle \mathbf{u}'(\mathbf{x}, t) \cdot \mathbf{u}'(\mathbf{x}, t + \tau) \rangle d\tau, \quad (6)$$

so that for the turbulent magnetic Prandtl number is

$$P_{m,t} = \frac{\nu_t}{\eta_t} = \frac{2}{5} = 0.4. \quad (7)$$

This results is similar to that of Nakano et al. (1979) for the thermal Prandtl number.

Rüdiger (1989) lists a number of other approaches for calculating turbulent transport coefficients, which all yield Prandtl numbers around or below unity. One particular approach is the renormalization group analysis which was applied to turbulence by Forster et al. (1977) for the case of a passive scalar, and later by Fournier et al. (1982) to the case with magnetic fields. These results are valid in the long-time large-scale limit, and the value of $P_{m,t}$ turned out to be close to 0.7; see Eq. (23) of Fournier et al. (1982).

Kitchatinov et al. (1994) use a mixing length approximation where terms of the form $d/dt - \nu \nabla^2$ are replaced by τ_{corr}^{-1} , where τ_{corr} is the correlation time of the turbulence. They find $\nu_t = (4/15)\tau_{\text{corr}} u_{\text{rms}}^2$ and $\eta_t = (1/3)\tau_{\text{corr}} u_{\text{rms}}^2$, so $P_{m,t} = 4/5 = 0.8$. Yet another approach is the τ -approximation where triple correlations are replaced by a damping term that is proportional to the quadratic moments (e.g. Kleeorin et al. 1996, Blackman & Field 2002). Here no Fourier transformation in time is used. This gives, as before, $\eta_t = (1/3)\tau u_{\text{rms}}^2$ (where τ is now interpreted as a relaxation time), but $\nu_t = (2/15)\tau u_{\text{rms}}^2$, so $P_{m,t} = 2/5 = 0.4$. This is half the value obtained from the mixing length approximation, but the same as in Eq. (7).

The fact that in all these cases $P_{m,t}$ is less than unity can be traced back to the presence of the pressure term in the momentum equation. If this term is ignored (as in pressureless Burgers turbulence or 'burgulence') one always gets $P_{m,t} = 1$.

It is tempting to speculate that the discrepancy between the different analytic approaches is related to the validity of some idealizing assumptions made in order to apply the quasilinear and other approximations. Clearly, additional approaches are needed to get a more complete picture regarding the correct value of $P_{m,t}$. It is nevertheless encouraging that $P_{m,t}$ does not strongly deviate from unity.

In the remainder of this paper we estimate ν_t and η_t numerically by considering the decay of an initial large scale velocity or magnetic field, respectively, in the presence of small scale turbulence.

3. The model

The equations describing compressible isothermal hydro-magnetic flows with constant sound speed, c_s , are

$$\frac{D\mathbf{u}}{Dt} = -c_s^2 \nabla \ln \rho + \frac{\mathbf{J} \times \mathbf{B}}{\rho} + \mathbf{F}_{\text{visc}} + \mathbf{f}, \quad (8)$$

$$\frac{D \ln \rho}{Dt} = -\nabla \cdot \mathbf{u}, \quad (9)$$

$$\frac{\partial \mathbf{B}}{\partial t} = \nabla \times (\mathbf{u} \times \mathbf{B}) + \eta \nabla^2 \mathbf{B}, \quad (10)$$

where \mathbf{u} is the velocity, ρ the density, \mathbf{B} is the magnetic field, and $\mathbf{J} = \nabla \times \mathbf{B} / \mu_0$ is the current density with μ_0 being the vacuum permeability. The viscous force is

$$\mathbf{F}_{\text{visc}} = \nu \left(\nabla^2 \mathbf{u} + \frac{1}{3} \nabla \nabla \cdot \mathbf{u} + 2 \mathbf{S} \cdot \nabla \ln \rho \right), \quad (11)$$

where $S_{ij} = \frac{1}{2}(u_{i,j} + u_{j,i}) - \frac{1}{3} \delta_{ij} \nabla \cdot \mathbf{u}$ is the traceless rate of strain tensor.

We solve the equations using the Pencil Code¹, which is a memory-efficient sixth-order finite difference code using the $2N$ -RK3 scheme of Williamson (1980). For most of the simulations a resolution of 128^3 meshpoints is used, but in Sect. 5 a higher resolution of up to 512^3 meshpoints was necessary.

We focus on the case where the forcing, \mathbf{f} , occurs at a wavenumber around $k_f = 10$. The forcing is such that the turbulence is subsonic and nonhelical. We consider two different periodic initial conditions,

$$\mathbf{B} = (\cos k_1 z, 0, 0) B_0 \quad (\text{nonhelical}) \quad (12)$$

and

$$\mathbf{B} = (\cos k_1 z, \sin k_1 z, 0) B_0 \quad (\text{helical}), \quad (13)$$

where B_0 is the amplitude of the initial field. In the fully helical case one may expect a different decay time because the magnetic helicity is a conserved quantity in the limit of small magnetic diffusivity. For the velocity field we use similar initial conditions, but we do not expect this to be sensitive to helicity, because kinetic helicity is not conserved in the limit $\nu \rightarrow 0$, and would only be conserved in the unphysical case $\nu = 0$.

A detailed discussion of the initial conditions may at first glance appear somewhat surprising, because for forced turbulent flows the initial conditions are normally forgotten after about one turnover time. This is indeed the case for hydrodynamic turbulence, but not for hydro-magnetic turbulence if the magnetic field has net magnetic helicity. The reason is that, regardless of the level of turbulence, the net magnetic helicity can only change on the resistive time scale. Our results below confirm this and they are indeed in agreement with earlier model predictions (cf. Blackman & Brandenburg 2002). The situation would be different if the initial field was bi-helical, i.e. with oppositely helical contributions at different scales. This

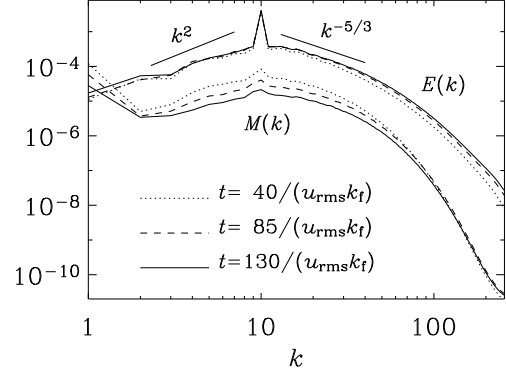


Fig. 1. Kinetic and magnetic energy spectra at three different times for a run with $\text{Re} = 150$ and $R_m = 15$.

case has been studied elsewhere (Yousef & Brandenburg 2003).

In Fig. 1 we show kinetic and magnetic energy spectra of the run with $\text{Re} = 150$ and $R_m = 15$ at three different times using a resolution of 512^3 meshpoints. The kinetic energy shows indications of a short inertial range in $15 < k < 40$. Below the forcing scale, in $2 < k < 9$, velocity and magnetic fields are random and δ -correlated in space, giving rise to a k^2 spectrum. The magnetic energy is substantially weaker than the kinetic energy. This is because here the magnetic Prandtl number is small, $P_m = 0.1$, and the magnetic Reynolds number is subcritical for dynamo action. With our definition of R_m the critical value lies around 25 (Haugen et al. 2003). The small scale magnetic energy is therefore maintained by constantly stirring the slowly decaying large scale field.

Given that the initial large scale field depends only on z , it makes sense to define a mean field by averaging over the x and y directions. Alternatively, one might define an average by Fourier filtering, but this has the disadvantage that not all the Reynolds rules are satisfied. For example, the average of a product of a mean and a fluctuating quantity would not vanish. However, for all practical purposes our horizontal average is nearly equivalent to a projection onto the $k = k_1$ Fourier mode. Indeed, the main reason for forcing at a large wavenumber, $k_f = 10$, is that we need some degree of scale separation. Without scale separation, there would be no way of distinguishing between mean and fluctuating fields. Since the velocity fluctuations are constantly driven via the forcing term, it would be impossible to measure any decay of the mean velocity. Nevertheless, even with scale separation there will always be a certain level of noise in the mean field whose energy is $(k_1/k_f)^2$ times smaller than energy of the fluctuations. This means that we can measure an exponential decay of the mean field only in a certain window where nonlinear effects are already weak, but were the noise level is not yet reached.

¹ <http://www.nordita.dk/data/brandenb/pencil-code>

4. Results

4.1. Decay of \bar{u} and \bar{B}

We begin by considering the decay of a helical large scale magnetic field and compare it with the decay of a large scale helical velocity field in a purely hydrodynamic simulation; see Fig. 2. Here, large scale velocity and magnetic fields are defined as horizontal averages over x and y ; the result is denoted by \bar{u} and \bar{B} , respectively. During the time interval when mean velocity and magnetic field decay exponentially, the corresponding decay rates are determined as

$$\lambda_u(\bar{u}) = \frac{d \ln \langle \bar{u}^2 \rangle^{1/2}}{dt}, \quad \lambda_B(\bar{B}) = \frac{d \ln \langle \bar{B}^2 \rangle^{1/2}}{dt}. \quad (14)$$

In the graphs of $\lambda_u(\bar{u})$ and $\lambda_B(\bar{B})$ an exponential decay shows up as a plateau. The magnetic field decay is initially slow, so $\lambda_B(\bar{B})$ is initially not constant, but then it speeds up and $\lambda_B(\bar{B})$ reaches a plateau. The decay of the velocity field is immediately fast and $\lambda_u(\bar{u})$ lies immediately on a plateau. This suggests that the turbulent magnetic diffusivity is affected by the strong initial field that in turn gives rise to a quenching of the turbulent magnetic diffusivity. Strong means that the magnetic field strength is comparable with the equipartition field strength, $B_{\text{eq}} = \langle \mu_0 \rho u^2 \rangle^{1/2}$. The initially strong large scale flow and the associated vorticity, on the other hand, do not and are also not expected to affect the turbulent viscosity and the associated decay of this large scale flow. For $|\bar{B}| \ll B_{\text{eq}}$, however, both \bar{u} and \bar{B} decay at the same rates, λ_u and λ_B , respectively. This allows us to calculate

$$\nu_t = \lambda_u / k_1^2, \quad \eta_t = \lambda_B / k_1^2, \quad (15)$$

where k_1 is the wavenumber of the initial large scale velocity and magnetic fields. From the present simulations, where $k_f/k_1 = 10$, we find

$$\nu_t \approx \eta_t = (0.8 \dots 0.9) \times u_{\text{rms}} / k_f \quad (\text{for } \bar{B}^2 \ll B_{\text{eq}}^2). \quad (16)$$

Once $|\bar{u}|$ has decreased below a certain level ($< 0.1 u_{\text{rms}}$), it cannot decay further and continues to fluctuate around $0.08 u_{\text{rms}}$, corresponding to the level of the rms velocity of the (forced!) turbulence at $k = k_1$ (see the dashed line in Fig. 2).

The quenching of the magnetic diffusivity, $\eta_t = \eta_t(\bar{B})$, can be obtained from one and the same run by simply determining the decay rate, $\lambda_B(\bar{B})$, at different times, corresponding to different values of $\bar{B} = |\bar{B}|$; see Fig. 3. To describe departures from purely exponential decay we adopt a \bar{B} -dependent η_t expression of the form

$$\eta_t(\bar{B}) = \eta_{t0} / (1 + a \bar{B}^2 / B_{\text{eq}}^2), \quad (17)$$

where η_{t0} is the unquenched (kinematic) value of η_t , described approximately by Eq. (16), and a is a fit parameter. According to Cattaneo & Vainshtein (1991) the parameter a is expected to be of the order of the magnetic

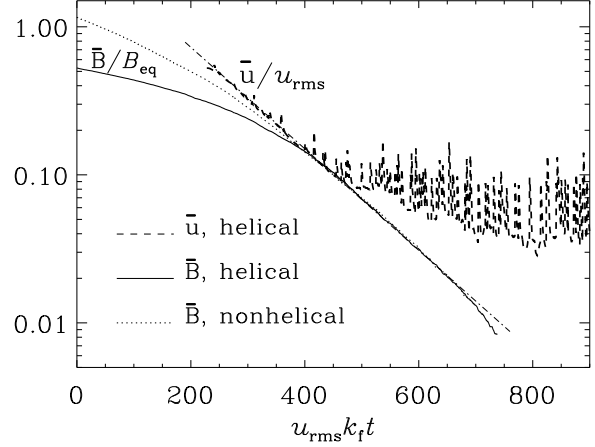


Fig. 2. Decay of large scale helical velocity and magnetic fields (dashed and solid lines, respectively). The graph of $\bar{u}(t)$ has been shifted so that both $\bar{u}(t)$ and $\bar{B}(t)$ share the same tangent (dash-dotted line), whose slope corresponds to $\nu_t = \eta_t = 0.86 u_{\text{rms}} / k_f$. The decay of a nonhelical magnetic field is shown for comparison (dotted line).

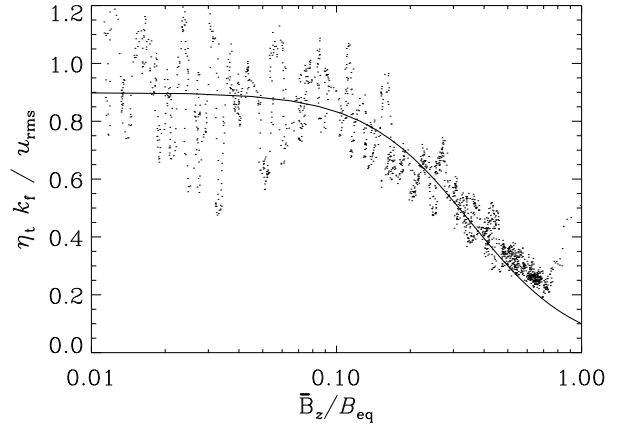


Fig. 3. Dependence of the turbulent diffusion coefficient on the magnitude of the mean field. The initial field is helical and corresponds to data points on the right hand side of the plot. $R_m \approx 20$. The data are best fitted by $a = 8 = 0.4 R_m$.

Reynolds number based on the microscopic magnetic diffusivity,

$$R_m = u_{\text{rms}} k_f / \eta. \quad (18)$$

Figure 3 suggests that $a \approx 0.4 R_m$.

Before we discuss the effective quenching behavior of η_t in more detail we should note that Eq. (17), and in particular the value of a , do not apply universally and depend on the field geometry. This is easily demonstrated by considering a nonhelical initial field. In that case the decay becomes unquenched already for $\bar{B}^2 / B_{\text{eq}}^2 \approx 1$. Equation (17)

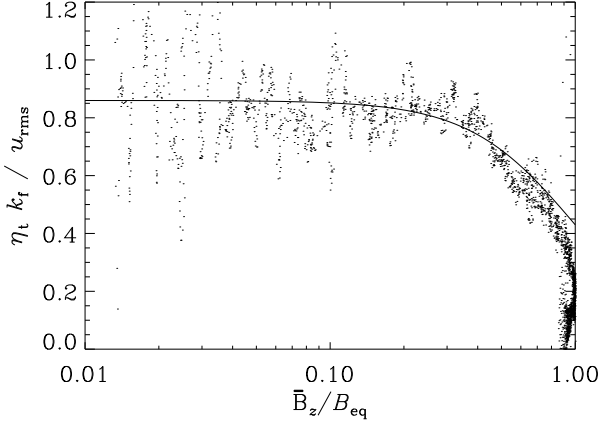


Fig. 4. Dependence of the turbulent diffusion coefficient on the magnitude of the mean field. The initial field is nonhelical. $R_m \approx 20$. The data are best fitted by $a = 1$, independent of R_m .

can still be used as a reasonable fit formula, but now $a = 1$ produces a good fit (independent of R_m); see Fig. 4.

In the nonhelical case there is an initial phase where the field increases due to the wind-up of the large scale field. Since we measure η_t from the decay rate of the large scale field, this would formally imply negative values of η_t . Traces of this effect can still be seen in Fig. 4 near $\bar{B}^2/B_{eq}^2 = 1$. For this reason our method can only give reliable results if $|\bar{\mathbf{B}}| \lesssim 0.8B_{eq}$. In the case of a helical initial field, on the other hand, we have $\bar{\mathbf{J}} \times \bar{\mathbf{B}} = 0$, i.e. the large scale field is force-free and interacts only weakly with the turbulence. In particular, there is no significant amplification from the initial wind-up of the large scale field.

4.2. Comparison with the dynamical quenching model

In the case of a helical field and for $\bar{B}^2/B_{eq}^2 \gtrsim R_m^{-1}$ the slow decay of $\bar{\mathbf{B}}$ is related to the conservation of magnetic helicity. As discussed already by Blackman & Brandenburg (2002), this behavior is related to the phenomenon of selective decay (e.g. Montgomery et al. 1978) and can be described by the dynamical quenching model. This model goes back to an early paper by Kleeorin & Ruzmaikin (1982, see also Kleeorin et al. 1995), but it applies even to the case where the turbulence is nonhelical and where there is no α effect in the usual sense. However, the magnetic contribution to α is still non-vanishing because it is driven by the helicity of the large scale field.

To demonstrate this quantitatively we solve, in the one mode approximation ($\mathbf{k} = \mathbf{k}_1$) with $\bar{\mathbf{B}} = \hat{\mathbf{B}} \exp(i\mathbf{k}_1 z)$, the mean-field induction equation

$$\frac{d\hat{\mathbf{B}}}{dt} = i\mathbf{k}_1 \times \hat{\mathcal{E}} - \eta k_1^2 \hat{\mathbf{B}} \quad (19)$$

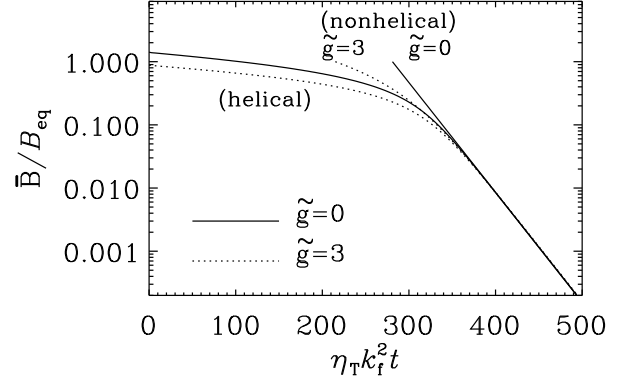


Fig. 5. Dynamical quenching model with helical and nonhelical initial fields. The quenching parameters are $\tilde{g} = 0$ (solid line) and 3 (dotted line). The graph for the nonhelical cases has been shifted in t so that one sees that the decay rates are asymptotically equal at late times.

together with the dynamical α -quenching formula [Eq. (13) of Blackman & Brandenburg (2002)]

$$\frac{d\alpha}{dt} = -2\eta k_f^2 \left(\alpha + \tilde{R}_m \frac{\text{Re}(\hat{\mathcal{E}}^* \cdot \hat{\mathbf{B}})}{B_{eq}^2} \right), \quad (20)$$

where

$$\hat{\mathcal{E}} = \alpha \hat{\mathbf{B}} - \eta_t i \mathbf{k}_1 \times \hat{\mathbf{B}} \quad (21)$$

is the electromotive force, and \tilde{R}_m is defined as the ratio η_{t0}/η , which is expected to be close to the value of R_m as defined by Eq. (18).

In Fig. 5 we show the evolution of \bar{B}/B_{eq} for helical and nonhelical initial conditions, $\hat{\mathbf{B}} \propto (1, i, 0)$ and $\hat{\mathbf{B}} \propto (1, 0, 0)$, respectively. In the case of a nonhelical field, the decay rate is not quenched at all, but in the helical case quenching sets in for $\bar{B}^2/B_{eq}^2 \gtrsim R_m^{-1}$.

In the helical case, the onset of quenching at $\bar{B}^2/B_{eq}^2 \approx R_m^{-1}$ is well reproduced by the simulations. In the nonhelical case, however, some weaker form of quenching sets in when $\bar{B}^2/B_{eq}^2 \approx 1$ (Fig. 4). We refer to this as standard quenching (e.g. Kitchatinov et al. 1994) which is known to be always present. In Blackman & Brandenburg (2002) this was modeled by allowing in Eq. (21) η_t to be \bar{B} -dependent. They adopted the formula

$$\eta_t = \eta_{t0} / (1 + \tilde{g} |\bar{\mathbf{B}}| / B_{eq}) \quad (22)$$

and found that, for a range of different values of R_m , $\tilde{g} = 3$ resulted in a good description of the simulations of cyclic $\alpha\Omega$ -type dynamos (Brandenburg et al. 2002). We emphasize that this η_t is *not* used in a diagnostic way as in Eq. (17), but rather in the numerical solution of Eqs (19) and (20). The resulting decay law, shown as a dotted line in Fig. 5, agrees now with the decay law seen in the turbulence simulations (Fig. 2). The helical case with $\tilde{g} = 3$ is still compatible with the simulations.

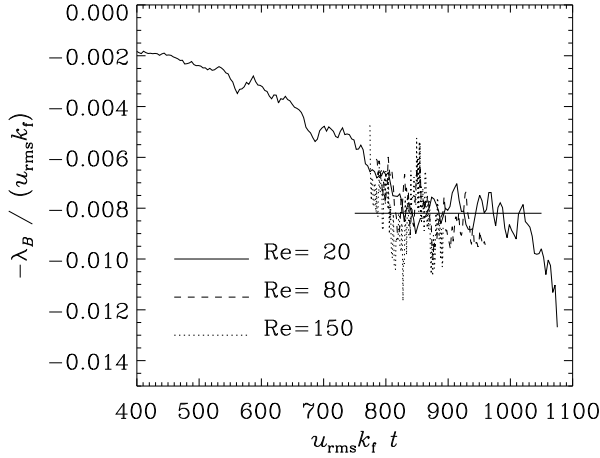


Fig. 6. Decay rate for three different values of Re and $R_m = 20$ (fixed), corresponding to values of $P_m = R_m/Re$ ranging from 0.1 to 1. All three curves have a plateau where the value of λ_B is the same. For $R_m = 80$ and 150 the graphs of λ_B have been shifted in t so that all three graphs show the plateau in approximately the same time interval.

5. Independence of microscopic viscosity

Finally we need to show that the turbulent magnetic Prandtl number is indeed independent of the microscopic magnetic Prandtl number. In Fig. 6 we plot the decay rates, obtained by differentiating $\ln \overline{B}(t)$, for three different values of the microscopic viscosity, keeping η fixed. The resulting values of the flow Reynolds number, $Re = u_{rms} k_f / \nu$, vary between 20 and 150, giving P_m in the range between 0.1 and 1. Within plot accuracy the three values of λ_B turn out to be identical in the interval where the decay is exponential.

The duration of this interval is $u_{rms} k_f \Delta t \approx 200$, which is comparable to the time interval in Fig. 2 during which the decay is exponential. In one of the three cases ($R_m = 20$) the initial field was rather strong, so that it takes a long time before the magnetic helicity constraint becomes unimportant so that the field can decay exponentially ($u_{rms} k_f t \approx 800$).

The numerical resolution used in most of the models is 128^3 mesh points. However, as Re is increased, higher resolution is required. For $Re=80$ we used 256^3 mesh points and for $Re=150$ we used 512^3 mesh points. This implies mesh a Reynolds number, $u_{rms} \Delta x / \nu$, based on the mesh spacing Δx , of about 18. Empirically we know that larger values are not generally possible.

6. Conclusions

The turbulence simulations presented here have shown that the turbulent magnetic Prandtl number is always of order unity, regardless of the values of the *microscopic* magnetic Prandtl number. Under the assumption of in-

compressibility, both the quasilinear approximation and the renormalization group approach give turbulent magnetic Prandtl numbers somewhat below unity, which is related to the pressure term in the momentum equation. Here we find instead $P_{m,t} \approx 1$. There are several plausible reasons for this discrepancy: (i) our simulations are actually weakly compressible, (ii) they are non-steady and, (iii) the idealizing assumptions made in the analytic approaches may not be justified.

Our results have also shown that, for nonhelical magnetic fields, the turbulent magnetic diffusivity is quenched when the magnetic energy becomes comparable to the kinetic energy. For helical magnetic fields, however, an apparent suppression of the decay rate is observed which agrees with predictions from a dynamical quenching model. If this suppression is described by an algebraic expression, quenching would set in for magnetic energies much below the kinetic energy.

The present work demonstrates that the dynamical quenching approach is not restricted to dynamos, but it can also deal with decay problems, as was already mentioned in Blackman & Brandenburg (2002). The dynamical quenching model is usually formulated in terms of α , but for helical mean fields \overline{J} and \overline{B} are parallel and the separation into contributions from $\alpha \overline{B}$ and $\eta_t \overline{J}$ becomes less meaningful. It is for this reasons that an α term appears in the description of the decay of helical fields, rather than a dynamical contribution to η_t -quenching.

The remaining quenching of η_t that affects both helical and nonhelical fields is consistent with an algebraic quenching formula that is non-catastrophic, i.e. independent of the microscopic magnetic diffusivity.

Although our results suggest that the turbulent magnetic Prandtl number is of order unity, we cannot claim that it is safe to use turbulent viscosity and magnetic diffusivity in a simulation of the dynamo or the magnetorotational instability, for example, as a replacement of a fully resolved simulation. First of all, the functional form of the turbulent transport coefficients is for realistic turbulent flows more complicated and involves in practice tensorial rather than scalar coefficients. Numerical evidence for this has been presented elsewhere in the context of shear flow turbulence (Brandenburg & Sokoloff 2002). Furthermore, there will be additional terms such as the α -effect (see Sect. 4.2) and the AKA-effect (Frisch et al. 1987; see also Brandenburg & Rekowski 2001). Most importantly, turbulent transport may be nonlocal, as is well known in meteorology when modeling atmospheric flows (Stull 1984, Ebert et al. 1989), where the turbulent transport is described by so-called transilient matrices (see also Miesch et al. 2000 for examples of astrophysical convection). Nonlocal transport means that the transport coefficients have to be replaced by integral kernels. In Fourier space, the convolution with an integral kernel corresponds to a multiplication with a wavenumber dependent factor. There is indeed some evidence that the main contribution comes only from the smallest wavenumbers (Brandenburg & Sokoloff 2002). This is primarily a consequence of a lack

of scale separation in naturally forced turbulence, such as shear flows or convection. In the present context, however, this is not an issue because we have deliberately considered the case where the scale of the turbulent eddies is much smaller than the scale of the large scale field ($k_f/k_1 = 10$).

Finally, we wish to point out that studies of instabilities (e.g. the magnetorotational or the dynamo instability) using turbulent transport coefficients can sometimes lead to paradoxical situations. In the case of solar convection, for example, one expects from mixing length theory that turbulent viscosity and thermal diffusivity are on the order of a few times $10^{12} \text{ cm}^2 \text{ s}^{-1}$. However, using such values in a global model of the sun leads to an instability (Rüdiger 1989, Rüdiger & Spahn 1992), which is in fact nothing but a repetition of the original convection instability that leads to turbulence in the first place (Tuominen et al. 1994). It is therefore plausible that the actual values of the turbulent transport coefficients should rather be close to the those for marginal stability. This would lead to a global constraint similar to the magnetic helicity constraint that governs the nonlinear behavior of the α -effect in helical hydromagnetic turbulence. At present, however, there is no theoretical framework that allows self-consistent modeling of convection using mean-field theory.

Acknowledgements. We thank an anonymous referee for making useful suggestions and drawing our attention to the paper by Fournier et al. (1982). Use of the supercomputers in Odense (Horseshoe), Trondheim (Gridur), and Leicester (Ukaff) is acknowledged.

References

Balbus, S. A., & Hawley, J. F. 1991, *ApJ*, 376, 214
 Balbus, S. A., & Hawley, J. F. 1998, *Rev. Mod. Phys.*, 70, 1
 Blackman, E. G., & Brandenburg, A. 2002, *ApJ*, 579, 359
 Blackman, E. G., & Field, G. B. 2002, *Phys. Rev. Lett.*, 89, 265007
 Bonanno, A., Elstner, D., Rüdiger, G., & Belvedere, G. 2002, *A&A*, 390, 673
 Brandenburg, A. 2001, *ApJ*, 550, 824
 Brandenburg, A., & Rekowski, B. v. 2001, *A&A*, 379, 1153
 Brandenburg, A., & Sokoloff, D. 2002, *Geophys. Astrophys. Fluid Dyn.*, 96, 319 (see also: [astro-ph/0111568](#))
 Brandenburg, A., Dobler, W., & Subramanian, K. 2002, *Astron. Nachr.*, 323, 99 (see also: [astro-ph/0111567](#))
 Cattaneo, F. 2003, in *Modelling of Stellar Atmospheres*, ed. N. E. Piskunov, W. W. Weiss, & D. F. Gray (Astron. Soc. Pac. Conf. Ser.) (in press)
 Cattaneo, F., & Vainshtein, S. I. 1991, *ApJ*, 376, L21
 Choudhuri, A.R., Schüssler, M., & Dikpati, M. 1995, *A&A*, 303, L29
 Christensen, U., Olson, P., & Glatzmaier, G. A. 1999, *Geophys. J. Int.*, 138, 393
 Dikpati, M., & Charbonneau, P. 1999, *ApJ*, 518, 508
 Ebert, E. E., Schumann, U., & Stull, R. B. 1989, *J. Atmosph. Sci.*, 46, 2178
 Frisch, U., She, Z. S., & Sulem, P. L. 1987, *Physica*, 28D, 382
 Forster, D., Nelson, D. R., & Stephen, M. J. 1977, *Phys. Rev. A* 16, 732

Fournier J.-D., Sulem P.-L., & Pouquet A. 1982, *J. Phys.*, A 15, 1392
 Haugen, N. E. L., Brandenburg, A., & Dobler, W. 2003, *ApJ*, 597, L141 (see also: [astro-ph/0303372](#))
 Kitchatinov, L. L., Rüdiger, G., & Pipin, V. V. 1994, *Astron. Nachr.*, 315, 157
 Kleeorin, N. I., & Ruzmaikin, A. A. 1982, *Magnetohydrodynamics*, 18, 116
 Kleeorin, N. I., Rogachevskii, I., & Ruzmaikin, A. 1995, *A&A*, 297, 159
 Kleeorin, N. I., & Mond, M., & Rogachevskii, I. 1996, *A&A*, 307, 293
 Kutzner, C., & Christensen, U. R. 2002, *Phys. Earth Planet. Int.*, 131, 29
 Miesch, M. S., Brandenburg, A., & Zweibel, E. G. 2000, *Phys. Rev. E* 61, 457
 Montgomery, D., Turner, L., & Vahala, G. 1978, *Phys. Fluids*, 21, 757
 Nakano, T., Fukushima, T., Unno, W., & Kondo, M. 1979, *PASJ*, 31, 713
 Noguchi, K., Pariev, V. I., Colgate, S. A., Beckley, H. F., & Nordhaus, J. 2002, *ApJ*, 575, 1151
 Roberts, P. H., & Soward, A. M. 1975, *AN*, 296, 49
 Roberts, P., & Stix, M. 1972, *A&A*, 18, 453
 Rüdiger, G. 1989, *Differential rotation and stellar convection: Sun and solar-type stars* (Gordon & Breach Science Publishers: New York)
 Rüdiger, G. & Shalybkov, D. 2002, *Phys. Rev. E*, 66, 016307
 Rüdiger, G., & Spahn, F. 1992, *Sol. Phys.*, 138, 1
 Rüdiger, G., Schultz, M., & Shalybkov, D. 2003, *Phys. Rev. E* 67, 046312
 Stull, R. B. 1984, *J. Atmosph. Sci.*, 41, 3351
 Tuominen, I., Brandenburg, A., Moss, D., & Rieutord, M. 1994, *A&A*, 284, 259
 Williamson, J. H. 1980, *J. Comput. Phys.*, 35, 48
 Yousef, T. A., & Brandenburg, A. 2003, *A&A*, 407, 7